CREATIVE SCIENCE

Journal home page: csj.snru.ac.th

Assessment of resistance spot welding parameters on the strength and reliability of AISI 316L stainless steel joints

Kannachai Kanlayasiri [a], Teerawut Khuenkaew [b], Phoometh Sangrayub [c] and Prajak Jattakul [d*]

[a] *Department of Industrial Engineering, School of Engineering, King Mongkut's Institute of Technology Ladkrabang, Bangkok, 10520, Thailand*

[b] *Department of Industrial Engineering, Faculty of Engineering, Rajamangala University of Technology Isan, Khon Kaen Campus, Khon Kaen, 40000, Thailand*

[c] *Department of Industrial and Production Engineering, Faculty of Engineering, Rajamangala University of Technology Rattanakosin, Prachuapkhirikhan, 77110, Thailand*

[d] *Department of Industrial Engineering, Faculty of Integrated Engineering and Technology, Rajamangala University of Technology Tawan-Ok, Chanthaburi, 22210, Thailand*

Article history:

Received: 26-03-2025
Revised : 01-05-2025
Accepted: 06-05-2025
Published: 08-05-2025
DOI : 10.55674/cs.v17i3.261405

Keywords:

Resistance spot welding;
Analysis of variance;
Reliability;
Weibull analysis;

Abstract

This study investigates how resistance spot welding parameters affect the joint strength and reliability of AISI 316L stainless steel, examining the effects of welding current, welding time, electrode pressure, and holding time. A 2^k full factorial design combined with Weibull analysis was employed to systematically evaluate the influence of each parameter. Results indicate that the optimal welding conditions—4.0 kA welding current, 0.5 s welding time, 0.3 MPa electrode pressure, and 5.0 s holding time—lead to superior joint strength and reliability, achieving an average tensile shear force of 2376.02 N. Examination of the welded specimens revealed a pull-out failure mode and ductile fracture. Unlike previous studies that primarily focused on maximizing strength, this research integrates both strength and reliability assessments, providing a more comprehensive evaluation. The Weibull analysis not only validates findings from conventional analysis of variance, but also provides additional insights into joint reliability, demonstrating an effective alternative methodology for optimizing welding parameters.

*** Corresponding author** : prajak_ja@rmutto.ac.th

1. Introduction

Stainless steel has long been utilized across various industries, with numerous grades finding applications in engineering due to their exceptional properties. Among them, austenitic stainless steels are particularly valued for their outstanding corrosion resistance, attributed to the presence of chromium and nickel. AISI 316L stainless steel, an austenitic variant, stands out as a widely used material in welding applications because of its low carbon content (less than 0.03%), which significantly reduces the risk of sensitization the precipitation of chromium carbides at grain boundaries during welding thereby enhancing its resistance to intergranular corrosion without requiring post-weld heat treatment [1]. Its fully austenitic microstructure also provides superior ductility, toughness, and resistance to cracking during welding processes. These metallurgical characteristics make 316L stainless steel highly compatible with various welding techniques, including metal inert gas (MIG) welding [2], tungsten inert gas (TIG)

welding [3], and resistance spot welding [4], making it an ideal choice for applications in the aerospace, medical, and chemical processing industries where both mechanical strength and corrosion resistance are critical.

Strength and reliability are closely related yet distinct concepts in welded joint evaluation. Strength refers to the maximum load a welded joint can withstand before failure, typically measured in terms of tensile shear force. Reliability, on the other hand, represents the consistency of this performance across multiple welds—essentially the probability that a joint will perform as expected under given conditions.

Resistance spot welding is a fusion welding method that employs heat and pressure to join metal sheets. During this process, welding heat originates from the contact resistance between the metal sheets forming a lap joint. This technique is widely and commonly used in various applications, and researchers have extensively examined the impact of welding parameters on the welded joint. Jagadeesha et al. [5] utilized the finite element method alongside experimental verification to explore the effects of welding current and time on nugget size and joint strength in resistance-spot welded 316L stainless steel. They concluded that increasing both welding parameters led to higher welding heat, larger nugget size, and greater joint strength. Hassoni et al. [6] utilized the design of experiments (DOEs) technique to investigate the influence of welding current, electrode pressure, squeeze time, and welding time on the tensile shear force of resistance-spot welded joints of 316L stainless steel. They identified the optimal welding conditions for achieving maximum joint strength. Vignesh et al. [7] investigated the optimal conditions for resistance spot welding parameters in the context of welding 316L stainless steel and 2205 duplex stainless steel using the Taguchi method. They pinpointed welding current as the most influential parameter for achieving maximum joint strength. Mansor et al. [8] studied the mechanical properties of micro-resistance spot welding between 316L stainless steel and Ti-6Al-4V alloy using DOEs. Among the parameters, welding current emerged as the most significant factor impacting joint strength. Vigneshkumar and Varthanan [9] used response surface methodology (RSM) and artificial neural networks (ANNs) to identify the optimal welding conditions for achieving maximum tensile shear force in spot-welded 304/316L stainless steel sheets. Their research indicated that ANNs outperformed RSM in predicting joint strength. Safari et al. [10] employed DOEs with Box-Behnken design to investigate the effects of resistance spot welding parameters on the joint strength of 201 stainless steel. Their findings highlighted welding current, welding time, electrode force, and cooling time as significant parameters impacting joint strength. Ravichandran et al. [11] utilized DOEs and RSM to study and optimize resistance spot welding parameters to achieve the maximum tensile shear force of welded joints in 1018 carbon steel and 430 stainless steel. Cao et al. [12] optimized resistance spot welding parameters for shear strength in welded joints between aluminum and Al-Si coated boron steel using RSM and genetic algorithms. They determined that welding current, welding time, and electrode pressure significantly influenced shear strength.

From the existing literature, it is evident that numerous techniques have been employed to investigate the impact of resistance spot welding parameters on joint strength. However, while joint reliability is critically important in engineering components, little has been published regarding the reliability of resistance spot-welded joints. Reliability studies have been reported for other welding techniques, such as friction stir welding [13, 14], and friction stir spot welding [15–17].

This article delves into the effects of resistance spot welding parameters on both the joint strength and the reliability of AISI 316 stainless steel. The study encompasses welding current, welding time, electrode pressure, and holding time. Employing the Weibull analysis, the tensile shear force of welded joints under various welding conditions is assessed, and the influence of welding parameters on joint strength and reliability is explored. Additionally, the failure mode, macrostructure, and microstructure of the welded specimens are investigated.

2. Materials and Methods

Material and experimental procedure

In this experiment, the chemical composition of the AISI 316L stainless steel was presented in Table 1. and a rectangular sheet of AISI 316L stainless steel measuring 76 mm x 19 mm x 0.5 mm was prepared per the AWS C3 standard for lap joint spot welding. Prior to welding, thorough surface cleaning was performed. Additionally, any organic and inorganic contaminants were removed using acetone/ethanol cleaning followed by ultrasonic cleaning. The welding process was carried out using a DC spot welding machine (Fan model ISO 25510522). Four welding parameters were investigated, namely welding current (A), welding time (B), electrode pressure (C), and holding time (D). The specific welding parameters and their corresponding settings are detailed in Table 2. The experiment utilized a 2^k factorial design, producing 16 different welding conditions. Each condition was tested with two replicates, resulting in a total of 32 welded specimens for analysis.

Table 1 Chemical composition of the AISI 316L Stainless steel

Chemical composition (wt%)									
C	Si	Mn	P	S	Cr	Ni	Mo	N	Fe
0.022	0.5	1.77	0.039	0.002	17.1	10.00	2.04	0.038	Base

Table 2 Welding parameters and their setting levels

Welding parameters	Low level	High level
A: Welding current (kA)	2.0	4.0
B: Welding time (s)	0.5	2.0
C: Electrode pressure (MPa)	0.3	0.5
D: Holding time (s)	0.0	5.0

The selection of the welding parameter ranges was carefully determined based on preliminary trials to ensure proper weld formation. Specifically, for welding current, the lower limit (2.0 kA) was chosen to provide sufficient heat input to form a weld nugget without causing incomplete fusion. The upper limit (4.0 kA) was selected to generate a larger nugget size and higher joint strength without risking overheating, molten metal expulsion, or severe surface deformation. Other parameters, including welding time, electrode pressure, and holding time, were similarly set based on preliminary experimental results to ensure stable weld quality and consistent joint performance.

The resistance spot-welded specimens underwent testing for tensile shear force using a Shimadzu universal testing machine (model AGX-100 kN) operated at a traverse speed of 10 mm/min. Furthermore, the microstructural examination of the welded joints was conducted using a JEOL scanning electron microscope (model JSM-6610LV). The fractured surface of the welded joint was closely examined to determine the fracture mode.

The Weibull analysis

Weibull analysis was employed to evaluate the impact of welding parameters on the strength and reliability of welded joints. As a statistical method based on the Weibull distribution, it enables the assessment of failure probability and material reliability. By analyzing tensile shear force data, the method provided valuable insights through probability plots, cumulative failure curves, survival functions, and hazard functions, thereby offering a comprehensive understanding of the welded joint behavior under stress. The formula for the two-parameter Weibull probability distribution function is expressed in Equation (1).

$$f(x;\alpha,\beta) = \left(\frac{\beta}{\alpha}\right)\left(\frac{x}{\alpha}\right)^{\beta-1} e^{-\left(\frac{x}{\alpha}\right)^{\beta}};\ (x \geq 0, \alpha > 0, \beta > 0) \quad (1)$$

The formula for the cumulative distribution function, used to depict the probability of failure of the welded joint, *F(x; α, β)*, at a tensile shear load of x, is expressed in Equation (2). The probability of survival, *R(x; α, β)*, is described in Equation (3). Furthermore, the formula for the hazard function of the Weibull distribution, *h(x; α, β)*, is presented in Equation (4). The hazard function serves as an indicator of the failure rate at a given tensile shear load.

$$F(x;\ \alpha,\beta) = 1 - e^{-\left(\frac{x}{\alpha}\right)^{\beta}} \quad (2)$$

$$R(x;\ \alpha,\beta) = 1 - F(x;\ \alpha,\beta) = e^{-\left(\frac{x}{\alpha}\right)^{\beta}} \quad (3)$$

$$h(x;\alpha,\beta) = \left(\frac{\beta}{\alpha}\right)\left(\frac{x}{\alpha}\right)^{\beta-1} \quad (4)$$

For the equations mentioned above, α represents the scale parameter, or characteristic strength, which signifies the 63.2 percentile value in the distribution. Meanwhile, β stands for the shape parameter of the distribution function. The shape parameter, or Weibull modulus, is employed to determine the material's reliability [18, 19]. A higher Weibull modulus indicates greater reliability of the specimen. In engineering applications, the Weibull modulus should typically exceed three [13].

3. Results and Discussion

Resistance spot-welded joints, subjected to various welding conditions, underwent tensile testing until failure, and the corresponding tensile shear forces were recorded. The welding parameters are presented in coded units of -1 and 1, representing low and high levels, respectively. The sequencing of the welding runs was randomly assigned to mitigate the influence of nuisance variables within the experiment.

Conventional analysis of variance

The analysis of variance (ANOVA) presented in Table 3 reveals that the welding current (A), electrode pressure (C), and their interaction (A*C) significantly influence the tensile shear force of the welded joint (p-values < 0.05), whereas the welding time (B), holding time (D), the two-way interactions A*B, A*D, B*C, B*D, the three-way interactions, and the four-way interaction do not show a statistically significant impact (p-values > 0.05). Based on the ANOVA results, as well as the main effects and interaction plots shown in Figures 1(a) and 1(b), the optimal welding condition appears to involve a high welding current and low electrode pressure, yielding a mean shear force of 2379.25 N. This conclusion holds true regardless of the choices made for other parameters, given that welding time and holding time are statistically insignificant. Typically, in ANOVA, low conditions of insignificant variables are selected to minimize operational costs. Consequently, the initial optimal welding condition would be a high welding current (4 kA), short welding time (0.5 s), low electrode pressure (0.3 MPa), and short holding time (0 s), represented by the condition (1, -1, -1, -1).

Table 3 Analysis of variance for tensile shear force

Source	DF	Adj SS	Adj MS	F-Value	P-Value
Model	15	6545716	436381	16.91	<0.001
Linear	4	5785609	1446402	56.03	<0.001
A	1	4396071	4396071	170.30	<0.001
B	1	16654	16654	0.65	0.434
C	1	1368775	1368775	53.03	<0.001
D	1	4109	4109	0.16	0.695
2-Way Interactions	6	557802	92967	3.60	0.019
A*B	1	50270	50270	1.95	0.182
A*C	1	425807	425807	16.50	0.001

Table 3 (continued) Analysis of variance for tensile shear force

Source	DF	Adj SS	Adj MS	F-Value	P-Value
A*D	1	4154	4154	0.16	0.694
B*C	1	23758	23758	0.92	0.352
B*D	1	35587	35587	1.38	0.258
C*D	1	18226	18226	0.71	0.413
3-Way Interactions	4	201595	50399	1.95	0.151
A*B*C	1	55830	55830	2.16	0.161
A*B*D	1	5005	5005	0.19	0.666
A*C*D	1	55537	55537	2.15	0.162
B*C*D	1	85222	85222	3.30	0.088
4-Way Interactions	1	710	710	0.03	0.870
A*B*C*D	1	710	710	0.03	0.870
Error	16	413011	25813	-	-
Total	31	6958727	-	-	-

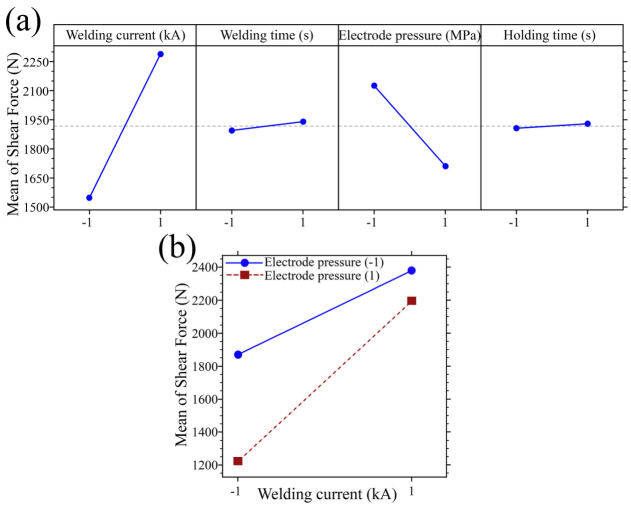

Fig. 1 (a) Main effects plot for tensile shear force of welded joint and (b) interaction plot between welding current and electrode pressure

Effect of welding current

The tensile shear force data was classified into two groups: low and high welding currents, without regard to the configurations of other parameters. These two sets of tensile shear forces, based on welding current, were subsequently analyzed for joint reliability using Minitab software. As depicted in the Weibull probability plot in Fig. 2, the shape parameter, or the Weibull modulus, for joints welded under high welding current was notably greater than that for joints welded under low welding current. This observation suggests that joints welded with high welding current exhibit higher reliability compared to those welded with low welding current. Furthermore, the scale parameter, or characteristic strength, for high welding current was significantly higher than that for low welding current, indicating that the 63.2 percentile of joints welded with high current fails at a higher shear load than their low current counterparts. This can be attributed to the fact that a higher welding current generates elevated welding heat, resulting in a larger weld nugget and consequently providing the welded joint with increased strength and reliability. Fig. 2(a) also suggests that approximately 1% of welded joints produced using a low welding current will fail under a shear load of approximately 690 N, while those welded by a high welding current will exhibit failure at around 1850 N.

As demonstrated in the cumulative failure, survival, and hazard plots, it is evident that joints welded with high welding current withstand a greater shear load before failing in comparison to those welded with low current. Based on this reliability analysis, it is recommended to employ a high welding current for achieving high-strength and reliable joints in 316L stainless steel.

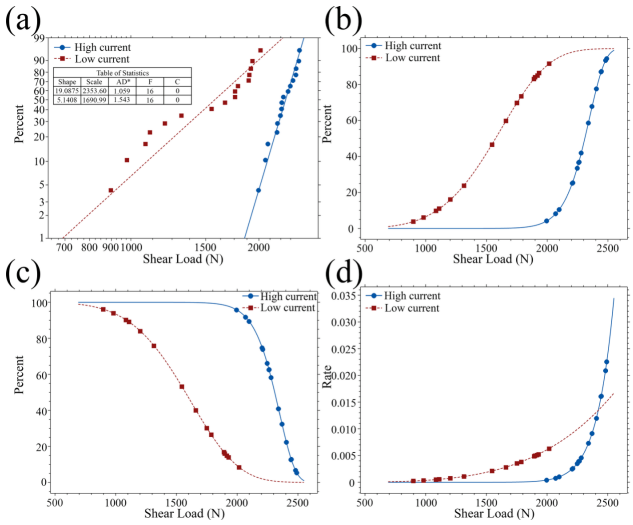

Fig. 2 (a) Weibull probability plot (b) cumulative failure plot (c) survival plot and (d) hazard plot for effect of welding current

Effect of welding time

To investigate the influence of welding time on the strength and reliability of welded joints in 316L stainless steel, all datasets were divided into two groups: long and short welding times, regardless of other parameter settings. The Weibull probability plot for welding times is presented in Fig. 3. In the probability plot, the shape and scale parameters for both long and short welding times appeared to be quite similar. Consequently, chi-square tests were conducted to ascertain whether they were statistically equivalent. As indicated in Table 4, the p-values for the chi-square tests exceeded the significance level (0.05) in both cases. This suggests that the shape and scale parameters for long and short welding times were not statistically different. Furthermore, the cumulative failure and survival plots for both welding times exhibited a resemblance. This made it challenging to definitively favor one welding time over the other.

However, a closer examination of the hazard plot in Fig. 3(d) revealed that the short welding time yielded a lower failure rate at a higher shear load. Hence, selecting a shorter welding time is advisable for achieving a more reliable joint. The reason why the longer welding time may result in a less reliable joint is that the chosen longer duration might exceed the optimal welding time, generating excessive heat and causing the expulsion of molten metal during welding. This, in turn, leads to reduced joint strength and reliability. Excessive welding time typically generates excessive heat and molten metal expulsion, which ultimately results in a weaker joint [20]. It is worth noting that, on average, the Weibull modulus and scale parameter of welding current (as in Fig. 1(a)) were higher than those of welding time (as in Fig. 3(a)), aligning with Joule's law ($Q = I^2Rt$) in which welding time (t) has a lesser impact on welding heat (Q) compared to welding current (I).

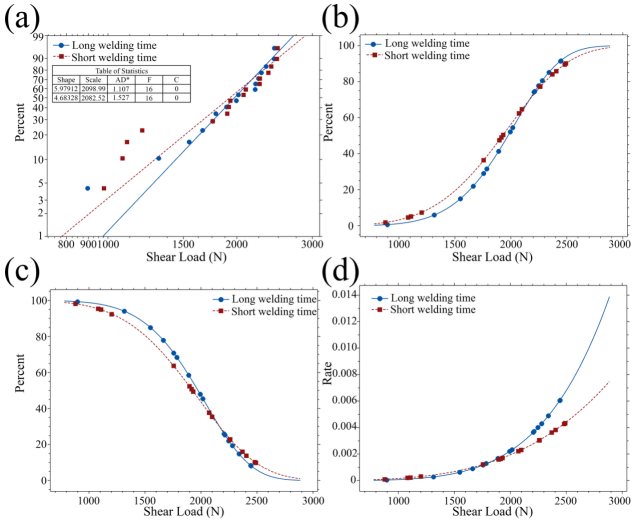

Fig. 3 (a) Weibull probability plot (b) cumulative failure plot (c) survival plot and (d) hazard plot for effect of welding time

Table 4 Test for shape and scale parameters

Test for equal shape parameters			Test for equal scale parameters		
Chi-square	**DF**	**p-value**	**Chi-square**	**DF**	**p-value**
0.656719	1	0.418	0.0123679	1	0.911

Effect of electrode pressure

To assess the impact of electrode pressure on joint reliability, the experimental data was processed similarly to the first two parameters. The effect of electrode pressure on joint reliability is depicted in the Weibull plot in Fig.

4. It is evident that the Weibull modulus for low electrode pressure is notably higher than that for high electrode pressure, indicating a more reliable welded joint. Additionally, the scale parameter, which signifies the 63.2 percentile value of shear load for low electrode pressure, is significantly greater than that for high pressure. This can be explained by the fact that welding under low pressure results in less intimate contact between the stainless steel sheets, leading to higher contact resistance and, consequently, increased welding heat. This, in turn, results in a larger weld nugget and a greater load-bearing capacity. In Fig. 4(a), it is also evident that approximately 1% of joints, which were welded using both low and high electrode pressure, will experience failure when subjected to shear loads of approximately 1370 N and 568 N, respectively.

Furthermore, the cumulative failure, survival, and hazard plots illustrate that the joint welded with low electrode pressure maintains its integrity under low shear load and fails only when subjected to high shear load. In contrast, the welded joint with high electrode pressure initiates failure even under low shear loads. Based on this reliability analysis, it is recommended to use low electrode pressure for the production of high-strength and reliable joints in 316L stainless steel.

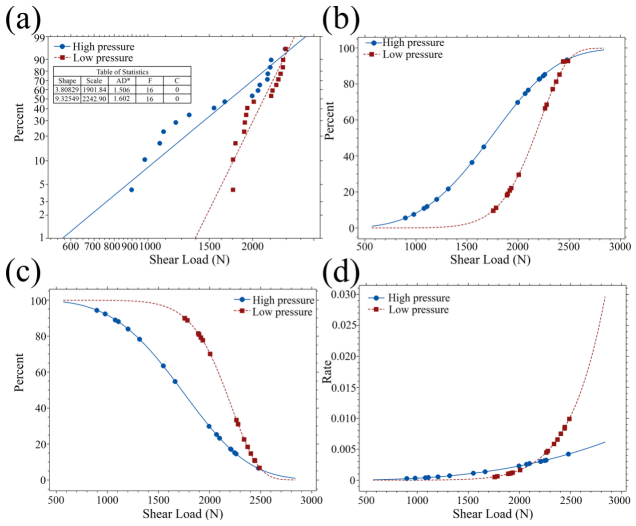

Fig. 4 (a) Weibull probability plot (b) cumulative failure plot (c) survival plot and (d) hazard plot for effect of electrode pressure

Effect of holding time

Holding time is the duration between the end of the welding current application and the release of electrode pressure on the specimens. In this experiment, we employed two holding time configurations: a long holding time of 5 seconds and a short holding time of 0 seconds. The Weibull probability plot reveals that the shape and scale parameters for both the long and short holding times are similar. To confirm the equality of these parameters, we conducted Chi-square tests, and the p-values for both tests exceeded the significance level of 0.05, as illustrated in Table 5. This suggests that the shape and scale parameters for both holding times are statistically equivalent. In Fig. 5, while the cumulative failure and survival plots indicate that the failure rate for the long holding time configuration is similar to that of the short holding time, more insight emerges from the hazard plot. This plot demonstrates that, for shear loads greater than approximately 1600 N, the long holding time results in a lower failure rate. This observation suggests that maintaining electrode pressure after the welding process enhances the bonding quality between the specimens. Based on these findings, employing a longer holding time to achieve more reliable joint formations is recommended.

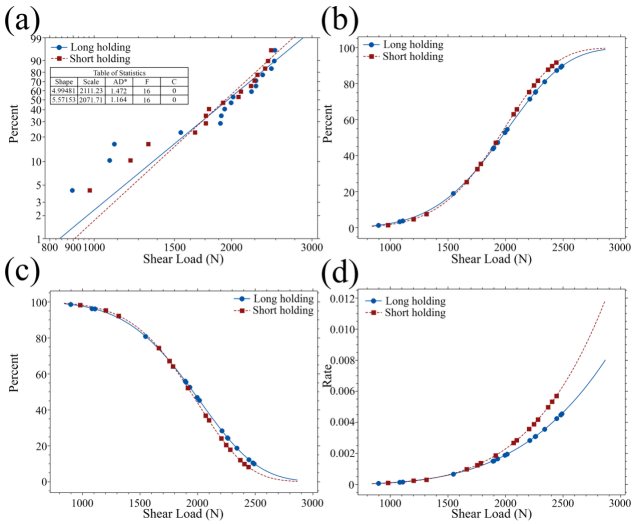

Fig. 5 (a) Weibull probability plot (b) cumulative failure plot (c) survival plot and (d) hazard plot for effect of holding time

Table 5 Test for shape and scale parameters

Test for equal shape parameters			Test for equal scale parameters		
Chi-square	**DF**	**p-value**	**Chi-square**	**DF**	**p-value**
0.130594	1	0.718	0.0725805	1	0.788

When considering the joint reliability information from the Weibull analysis, the optimal welding condition differs. While conventional ANOVA primarily focuses on the influence of welding variables on the measured outcome, the Weibull analysis provides additional insights for selecting the appropriate levels of insignificant variables. These insights can be derived from various plots, including cumulative failure, survival, and hazard plots.

Drawing from the enhanced insights provided by the Weibull analysis, the recommended welding configuration features a high welding current (4 kA), short welding time (0.5 s), low electrode pressure (0.3 MPa), and a long holding time (5 s), represented by the condition (1, -1, -1, 1). This configuration not only ensures high strength but also improves the overall reliability of the joint as confirmed in section of macro and microstructure of welded specimens.

Macro and microstructure of welded specimens

Figure 6 displays the failure mode of specimens welded under different welding conditions. Both specimens failed in a pull-out mode, indicating that they were correctly welded under both welding conditions. This mode of failure is preferred over the interfacial mode, which would suggest that the specimens were not sufficiently fused to form a complete weld nugget. In such cases, only interfacial bonding between the specimen surfaces occurs, resulting in a weaker joint. Incomplete joining may be due to inappropriate welding conditions and/or surface preparation.

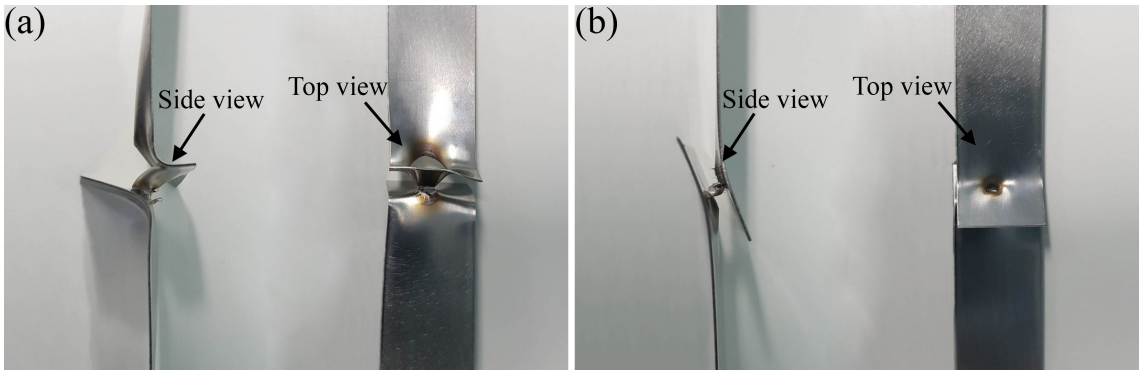

Fig. 6 Failure of the specimens welded at (a) 4 kA, 0.5 s, 0.3 MPa, 5 s and (b) 4 kA, 0.5 s, 0.3 MPa, 0 s

Dashed lines in Figures 7(a) and (b) outline the perimeter of the weld nugget obtained from the (1, -1, -1, 1) and (1, -1, -1, -1) welding conditions, respectively. It is evident that the (1, -1, -1, 1) condition produces a larger weld nugget than the opposite welding condition, resulting in a higher strength and more reliable joint. Both weld nuggets exhibit a similar microstructure characterized by columnar grains, which is typical in spot welding of 316L stainless steel [21, 22].

It is worth noting that there is a void at the center of the weld nugget obtained from the (1, -1, -1, -1) welding condition. This void significantly compromises joint strength and reliability by reducing the load-bearing area during tensile shear tests. The void results from the zero holding time during welding. The presence of a void at the center of the weld nugget observed under the 0 s holding time condition can be attributed to the lack of post-heating electrode pressure. Without sufficient holding time, the molten metal solidifies rapidly without being adequately

pressed, leading to thermal contraction and gas entrapment. Thermal contraction occurs as the molten metal cools and solidifies, causing volumetric shrinkage that, without sufficient holding pressure, creates voids primarily at the center of the weld nugget where solidification occurs last. Gas entrapment results when dissolved gases like hydrogen, nitrogen, and oxygen attempt to escape during cooling but become trapped within the rapidly solidifying metal matrix when adequate holding time is not provided. This incomplete consolidation decreases the load-bearing area of the weld and adversely affects both the tensile strength and reliability of the joint.

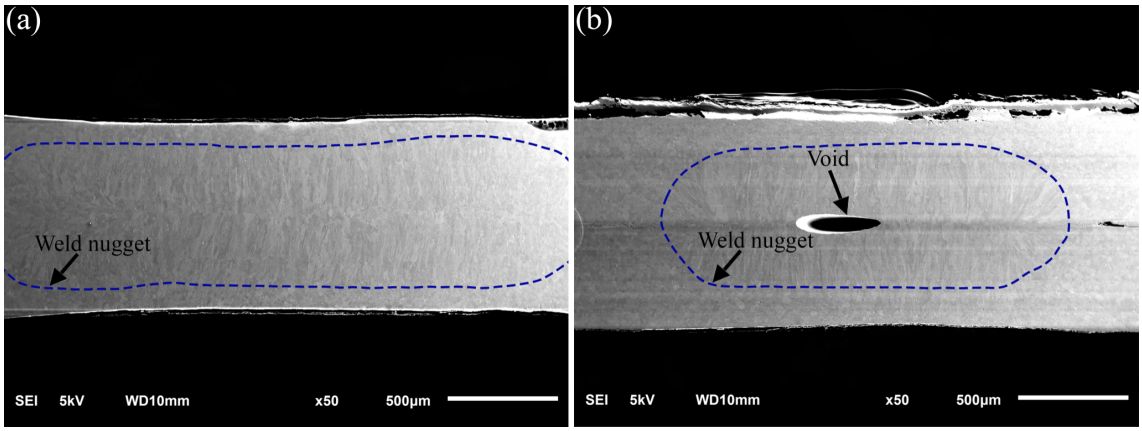

Fig. 7 Weld nugget of the specimens welded at (a) 4 kA, 0.5 s, 0.3 MPa, 5 s and (b) 4 kA, 0.5 s, 0.3 MPa, 0 s

Figure 8 presents the fractured surface of specimens welded under (1, -1, -1, 1) and (1, -1, -1, -1) conditions. Dimples are clearly visible on both fractured surfaces, indicating a ductile fracture in both specimens. Ductile fracture is preferable to brittle fracture in welded joints because it involves substantial plastic deformation before failure, making it easier to detect impending failure and prevent catastrophic damage. Despite the difference in the size of weld nuggets, both specimens exhibited a decent joint under both welding conditions.

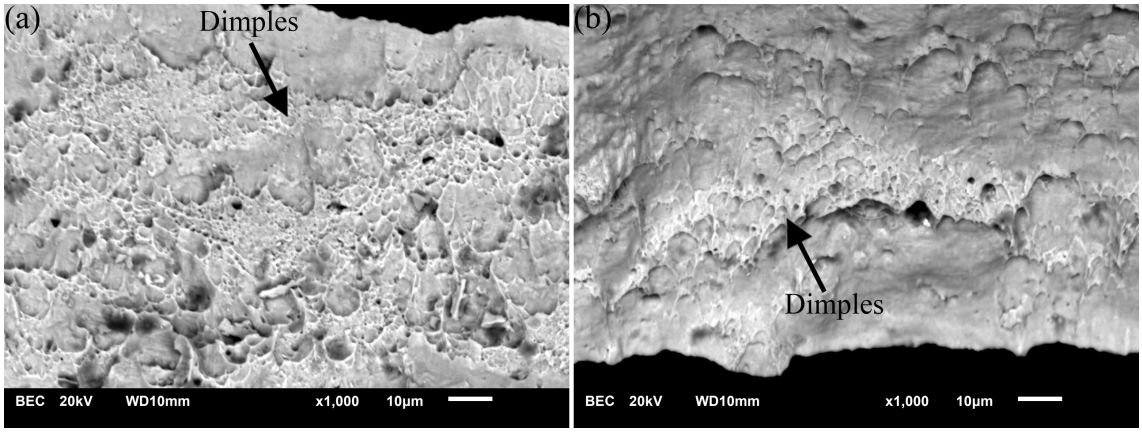

Fig. 8 Fractured surface of the specimens welded at (a) 4 kA, 0.5 s, 0.3 MPa, 5 s and (b) 4 kA, 0.5 s, 0.3 MPa, 0 s

The results of this study align with previous findings reported by Jagadeesha et al. [5], who observed that increasing welding current leads to higher joint strength due to larger nugget formation. Similarly, Hassoni et al. [6] also identified welding current and electrode pressure as significant factors influencing the tensile shear strength of 316L stainless steel spot welds, which is consistent with the ANOVA results presented in this study. However, unlike previous studies that primarily focused on maximizing joint strength, this research additionally incorporated Weibull analysis to assess joint reliability, offering a more comprehensive evaluation. While Vignesh et al. [7] emphasized the importance of welding current in achieving maximum joint strength using Taguchi methods, they did not consider reliability aspects, which are crucial for ensuring consistent performance in real-world applications. Therefore, compared to earlier works, this study advances the understanding of resistance spot welding of 316L stainless steel by jointly optimizing strength and reliability, rather than focusing solely on strength.

The findings are applicable to industries requiring reliable stainless steel welds, such as automotive, aerospace, and medical manufacturing sectors. However, the results are specific to the tested material thickness and joint configuration; further studies should explore applicability across different stainless steel grades, thicknesses, and environmental conditions to fully generalize these findings.

4. Conclusions

In this study, the influence of resistance spot welding parameters on the joint strength and reliability of AISI 316L stainless steel was investigated using Weibull analysis. It was found that welding with a high welding current (4.0 kA), short welding time (0.5 s), low electrode pressure (0.3 MPa), and long holding time (5.0 s) yields higher joint strength and reliability compared to the condition identified by conventional ANOVA (4.0 kA welding current, 0.5 s welding time, 0.3 MPa electrode pressure, and 0 s holding time). Specifically, these optimal conditions produced an average tensile shear force of 2376.02 N and enhanced reliability, as confirmed by Weibull analysis.

The Weibull analysis enabled a simultaneous assessment of joint strength and reliability, offering additional insights compared to conventional ANOVA, which only focuses on joint strength. The results obtained from the Weibull analysis primarily align with those of conventional ANOVA in terms of the influence of welding parameters on joint strength. However, the combined use of the Weibull analysis and ANOVA allows for a more comprehensive understanding of the effects of process parameters on the response, aiding in the selection of the proper welding condition. Macro and microstructure analyses revealed that the suggested welding condition resulted in a joint that failed in a pull-out mode with a ductile fractured surface, and the weld nugget was larger than that of the ANOVA welding condition.

The integration of ANOVA and Weibull analysis in this study allowed for a comprehensive evaluation of both joint strength and reliability. While ANOVA identified the significant welding parameters affecting average tensile strength, Weibull analysis offered additional insights into the variability and probability of failure, leading to a more informed selection of optimal welding conditions for industrial applications.

5. Acknowledgement

This work was financially supported by King Mongkut's Institute of Technology Ladkrabang [Grant number A118-0460-002].

6. References

[1] Weman, K. (2011). *Welding processes handbook* (2nd ed.). Woodhead Publishing Cambridge, UK.

[2] Ghosh, N., Pal, P.K., & Nandi, G. (2016). Parametric Optimization of MIG Welding on 316L Austenitic stainless steel by grey-based taguchi method. *Procedia Technology*, *25*, 1038–1048. https://doi.org/10.1016/j.protcy.2016.08.204

[3] Ghumman, K.Z., Ali, S., Din, E.U., Mubashar, A., Khan, N.B.,&Ahmed, S.W. (2022). Experimental investigation of effect of welding parameters on surface roughness, micro-hardness and tensile strength of AISI 316L stainless steel welded joints using 308L filler material by TIG welding. *Journal*

of Materials Research and Technology, *21*, 220–236. https://doi.org/10.1016/j.jmrt.2022.09.016

[4] Krishnan, V., Ayyasamy, E., Paramasivam, & V. (2021). Influence of resistance spot welding process parameters on dissimilar austenitic and duplex stainless steel welded joints. *Proceedings of the Institution of Mechanical Engineers, Part E: Journal of Process Mechanical Engineering 2021*, *235*, 12–23. https://doi.org/10.1177/0954408920933528

[5] Jagadeesha, T., & Jothi, T. J. S. (2017). Studies on the influence of process parameters on the AISI 316L resistance spot-welded specimens. *International Journal of Advanced Manufacturing Technology*. *93*, 73–88. https://doi.org/10.1007/s00170-015-7693-y

[6] Hassoni, S. M., Barrak, O. S., Ismail, M. I., & Hussein, S. K. (2022). Effect of welding parameters of resistance spot welding on mechanical properties and corrosion resistance of 316L. *Materials Research*, *25*(2), e20210117. https://doi.org/10.1590/1980-5373-MR-2021-0117

[7] Vignesh, K., Elaya Perumal, A., & Velmurugan, P. (2017). Optimization of resistance spot welding process parameters and microstructural examination for dissimilar welding of AISI 316L austenitic stainless steel and 2205 duplex stainless steel. *International Journal of Advanced Manufacturing Technology*, *93*, 455–465. https://doi.org/10.1007/s00170-017-0089-4

[8] Mansor, M. S. M., Yusof, F., Ariga, T., & Miyashita, Y. (2018). Microstructure and mechanical properties of micro-resistance spot welding between stainless steel 316L and Ti-6Al-4V. *International Journal of Advanced Manufacturing Technology*, *96*, 2567–2581. https://doi.org/10.1007/s00170-018-1688-4

[9] Vigneshkumar, M., & Varthanan, P. A. (2019). Comparison of RSM and ANN model in the prediction of the tensile shear failure load of spot welded AISI 304/316 L dissimilar sheets. *International Journal of Computational Materials Science and Surface Engineering*, *8*(2), 114–130. https://doi.org/10.1504/IJCMSSE.2019.102292

[10] Safari, M., Mostaan, H., Yadegari Kh, H., & Asgari, D. (2017). Effects of process parameters on tensile-shear strength and failure mode of resistance spot welds of AISI 201 stainless steel. *International Journal of Advanced Manufacturing Technology*, *89*, 1853–1863. https://doi.org/10.1007/s00170-016-9222-z

[11] Ravichandran, P., Anbu, C., Meenakshipriya, B., & Sathiyavathi, S. (2020). Process parameter optimization and performance comparison of AISI 430 and AISI 1018 in resistance spot welding process. *Materials Today: Proceedings*, *33*, 3389–3393, https://doi.org/10.1016/j.matpr.2020.05.197

[12] Cao, X., Li, Z., Zhou, X., Luo, Z., & Duan, J. (2021). Modeling and optimization of resistance spot welded aluminum to Al-Si coated boron steel using response surface methodology and genetic algorithm. *Measurement*, *171*, https://doi.org/10.1016/j.measurement.2020.108766

[13] Ku, M. H., Hung, F. Y., & Lui, T. S. (2019). The effect of hyper-rotation on the Weibull distribution of tensile properties in a friction stirred AA7075 aluminum alloy. *Materials Chemistry and Physics*, *226*, 290–295. https://doi.org/10.1016/j.matchemphys.2018.12.085

[14] Sohn, H. J., Haryadi, G. D., & Kim, S. J. (2014). Statistical aspects of fatigue crack growth life of base metal, weld metal and heat affected zone in FSWed 7075-T651 aluminum alloy. *Journal of Mechanical Science and Technology*, *28*, 3957–3962. https://doi.org/10.1007/s12206-014-0906-8

[15] Brzostek, R. C., Suhuddin, U., & Dos Santos, J. F. (2018). Fatigue assessment of refill friction stir spot weld in AA 2024-T3 similar joints. *Fatigue & Fracture of Engineering Materials & Structures*, *41*, 1208–1223. https://doi.org/10.1111/ffe.12764

[16] Effertz, P. S., Infante, V., Quintino, L., Suhuddin, U., Hanke, S., & Dos Santos, J. F. (2016). Fatigue life assessment of friction spot welded 7050-T76 aluminium alloy using Weibull distribution. *International Journal of Fatigue*, *87*, 381–390. https://doi.org/10.1016/j.ijfatigue.2016.02.030

[17] Lin, C. W., Hung, F. Y., Lui, T. S., & Chen, L. H. (2014). Weibull statistics of tensile-shear strength of 5083 aluminum alloy after friction stir spot welding. *Materials Transactions*, *56*(1), 54–60. https://doi.org/10.2320/matertrans.M2014281

[18] Yang, C. W., Hung, F. Y., Lui, T. S., Chen, L. H., & Juo, J. Y. (2009). Weibull statistics for evaluating failure behaviors and joining reliability of friction stir spot welded 5052 aluminum alloy. *Materials Transactions*, *50*(1), 145–151 https://doi.org/10.2320/matertrans.MRA2008341

[19] Lima, R. S., & Marple, B. R. (2003). Optimized HVOF titania coatings, *Journal of Thermal Spray Technology*, *12*, 360–369. https://doi.org/10.1361/105996303770348230

[20] Wang, Y. R., Mo, Z. H., Feng, J. C., & Zhang, Z. D. (2007). Effect of welding time on microstructure and tensile shear load in resistance spot welded joints of AZ31 Mg alloy. *Science and Technology of Welding and Joining*, *12*, 671–676. https://doi.org/10.1179/174329307X238380

[21] Kianersi, D., Mostafaei, A., & Amadeh, A. A. (2014). Resistance spot welding joints of AISI 316L austenitic stainless steel sheets: Phase transformations, mechanical properties and microstructure characterizations. *Materials & Design*, *61*, 251–263. https://doi.org/10.1016/j.matdes.2014.04.075

[22] Kim, S., Park, S., Kim, M., Kim, D. Y., Park, J., & Yu, J. (2023). Weldability of additive manufactured stainless steel in resistance spot welding. *Metals*, *13*, https://doi.org/10.3390/met13050837